Supporting Information

Righter and O'Brien 10.1073/pnas.1013480108

SI Text

Chemical and Physical State of Inner Solar System. Before we begin a detailed discussion of terrestrial planet formation, some background information is necessary. Some general trends among the terrestrial planets must be satisfied in any successful model or hypothesis for their formation. First, the two largest inner planets—Earth and Venus—are roughly similar in mass, while Mercury and Mars are each less than 1/10 of an Earth mass. The sizes of the planets' metallic cores, relative to silicate mantles, show a decrease with distance from the Sun, while the FeO content of their mantles increases (Fig. 1*A*). Eccentricities of the planets' orbits show a range of values with Mercury having the highest at 0.2056 and Venus having the lowest at 0.0068 (Fig. 1*B*). The inclination of the orbits of Earth and Venus, as referenced to the invariable plane (essentially the mean orbital plane of all the planets), are about 1.26 and 1.52 degrees, respectively, and 4.41 and 6.98 degrees for Mars and Mercury (Fig. 1*B*). And finally, it is worth mentioning that while Earth and Mars have similar rotational periods, Mercury has a slow rotational period (58 d) due to a spin-orbit resonance (three rotations for every two orbits around the Sun), and Venus has an even longer rotational period that is in the opposite direction to the other three planets (243 d). In addition to these characteristics of our own Solar System and inner planets, the characteristics (planet numbers, masses, inclinations, eccentricities, and orbital periods) of other solar systems may also be used to help constrain formation models, because a diversity of outcomes is possible and ours is just one of those.

Volatile Element Depletions. A general characteristic of differentiated bodies in the inner Solar System, as well as many of the chondritic meteorite groups, is their variable degrees of volatile element depletion (Fig. S2). This depletion is not well understood, and remains a considerable barrier to a complete understanding of terrestrial planet formation (see below). For example, samples from small differentiated bodies such as the angrites and eucrites, have very low contents of volatile elements, such as K and Na. These depletions cannot be attributed to volatile loss during magmatism or volcanism, nor to Rayleigh fractionation, because these processes would leave a distinct isotopic fingerprint that is not observed (1). Even the Earth and Mars are depleted in volatile elements relative to CI chondrites. The magnitude of the depletions scales with condensation temperature for these elements. As a result, most conclude that these volatile element depletions are due to either condensation or evaporation under near- equilibrium conditions (e.g., ref. 1). Such processes can operate on precursor materials in the nebula which are then later incorporated into larger bodies.

Chronology of Solar System. The timing of these different stages has received considerable quantitation from studies of various planetary and extraterrestrial materials (e.g., refs. 2–5). This discussion of timing should be predicated with a definition of T_0, which is the abbreviation for the age of oldest known solid material in the solar nebula (e.g., ~4,568 Ma; 3; Fig. 3). Similarly, chondrules formed early and also overlapped with the formation and earliest differentiation of planetesimal or small embryo-sized bodies, which took place within 3 Ma of T_0 (3, 4). Accretion of, and core formation in Mars, which is about a tenth the mass of the Earth, has been constrained to have been completed ~10 Ma after T_0 (2). Finally, the last giant impact on the Earth—which is also thought to have formed the Moon—occurred between ~50 and 150 Ma after T_0 (6). These geo-chronological constraints are in good agreement with the timing requirements that result from various kinds of physical and dynamic modeling of planetary formation processes.

Dust to Planetesimals: Mechanisms Impeded by Turbulence. In the case where there is no turbulence, 100 to 1,000 m sized bodies can form as quickly as 10^5 y by pairwise sticking (7, 8). Growth by gravitational instability can also occur rapidly, as particles settle into a thin layer at the midplane of the disk and grow into gravitationally bound clumps (9). However, both of these mechanisms are inefficient or fail in the presence of turbulence, so defining the nature and extent of turbulence is key to understanding conditions that foster growth. For example, coupling gas drag and eddies in a turbulent environment significantly increases particle velocities, especially as the bodies approach a size near 1 m. Under such circumstances, growth is impeded and collisions with smaller particles can lead to erosion (10). In the case of gravitational instability, as particles settle into a layer at the midplane of the disk, they begin to collectively move at the Keplerian velocity, while gas above and below the particle layer moves at a sub-Keplerian velocity because it is partially pressure supported. The mismatch in velocities between the gas and the dust layer leads to turbulence and vertical mixing (10), which prevents the particles from becoming concentrated enough for gravitational instability to occur.

Modelling Embryos to Planets. Early modeling efforts of this stage were somewhat limited by computational time and efficiency, and utilizing tens to ~100 particles of roughly equal size, could produce final planet mass distributions and total masses that were broadly similar to those in our Solar System (i.e., 3 to 4 planets; 11–13). However, the resulting planets generally had eccentricities and inclinations that were significantly higher than those observed in our system, and forming small Mars-like planets was generally difficult. Later efforts seized on and expanded several aspects of modeling that have strong controls on the final outcomes. Computational breakthroughs such as the increase in computer speed and the development of fast integration algorithms such as SyMBA and Mercury (14, 15) allowed the use of significantly larger numbers of bodies in the calculations ($N >= 1{,}000$ compared to ~100, e.g., refs. 16–18). Another new integration algorithm combines a statistical coagulation code for the growth and evolution of small bodies with an N-body integrator that treats the evolution of large embryos individually (19).

Homogeneous or Heterogeneous Accretion? Asteroid 4 Vesta is thought to be a differentiated body consisting of a core, mantle, and largely basaltic crust. Models advanced to explain the meteorite and astronomical data involve an initially chondritic body that was a mixture of carbonaceous and ordinary chondrite material (20). This material melted to form a magma ocean and small metallic core. The magma ocean then crystallized during continued cooling, resulting in the differentiated mantle and crust. This scenario is not strictly homogeneous accretion, because the bulk composition appears to be a mixture of C and O chondrites. But this mixture, and its cooling from a largely molten state, can explain the major and trace element and stable isotopic data and the rapid crystallization from a magma ocean and differentiation can explain the radiogenic isotopic data available for these meteorites.

Information available for Mars includes the 50+ martian meteorites as well as the data from many robotic missions to the surface and in orbit. The bulk composition of Mars is thought to be a mixture of ordinary and carbonaceous chondrites (21). A combination of siderophile elements, as well as radiogenic isotopic data (Sr, Nd, Hf, W) argue that Mars underwent early differentiation (e.g., refs. 2, 22), and the planet was hot enough to melt about halfway to the core-mantle boundary (23). Again, as for 4 Vesta, this body is comprised of a mixture of known chondritic material, and underwent a hot early differentiation, but at higher pressures than the asteroid.

Finally, we turn to the Earth for which there are many studies and therefore several ideas that are still debated (Fig. S6). Both heterogeneous accretion and homogeneous accretion models were based heavily on partitioning of siderophile (iron metal-loving) elements between core and mantle (metal and silicate), but lack of high pressure and temperature data for these elements always overshadowed the details of the results. More recent models for Earth have included many different siderophile elements (Ni, Co, Mo, W, P, Ga, Nb, Mn, V, Cr, Cu, Zn) and extended studies to the higher pressures and temperatures appropriate for melting of planetary interiors. The resulting models include two general end members: some that argue for a pressure and temperature range that can explain many elements simultaneously by deep metal-silicate equilibrium perhaps representing thermal conditions caused by the last large impact between Earth and Moon-forming impactor (24, 25). In this model, the more refractory siderophile elements (Ni, Co, Mo, and W) as well as eight additional siderophile elements are explained by metal-silicate equilibrium within Earth's interior (25), and the lower mantle is an important reservoir for Nb, Mn, V, and Cr.

Another kind of model considers smaller groups of elements (Cr, Mn, V, and Nb among others), and assumes early reduced core formation (at 40 to 70 GPa and 3,000–4,000 K), followed by a later oxidized condition (26), similar to the heterogeneous accretion models of several decades ago. The latter model also results in very high pressure and temperature conditions, because it is assumed that the core is the main reservoir for Nb, Mn, V, and Cr (26). Ongoing studies should help resolve which model is more robust, and also provide constraints on the identity of the light element in Earth's core (S, C, O, Si, or H).

Habitability. An origin from comets has long been an explanation for Earth's water, but the realization that Earth's oceans have a significantly lower D/H (deuterium/hydrogen) ratio that water in comets, however, has prompted reexamination of this idea, even though the D/H measurements are only from a few comets so far (27). Another more solid argument against comets as a primary source is their very low dynamical delivery efficiency—they could account for at most about 10% of Earth's water (28). If planetesimals grew fast enough so that they could store some water away (e.g., ref. 29) the water could have been acquired directly from the solar nebula (27). A topic that has received much attention in the past several years is how much water could be present in planetary embryos and how many could be water-bearing? Some carbonaceous chondrites, presumably from the outer asteroid belt, have up to 10% water by mass, and some have been metamorphosed and still retain several wt% water [e.g., Rchondrite LAP 04840; (30)]. One embryo alone could come from the outer asteroid belt and deliver all of (or more than) Earth's water (28). And the thermal and dynamical environment may also play a role in water delivery. For example, the location of the snow line in the nebula, and the presence or absence of giant planets, may play a critical role in the frequency of water-bearing Earth-sized planets.

With new appreciation of radial mixing in later stages of accretion, it is clear that terrestrial planets may be capable of containing several wt% water (31, 32). So, although all of Earth's water could have potentially come from embryos, the embryos themselves are mixtures of various sources, and Earth's water could have come from a combination of nebular sources, later embryos, and comets that are similar to the meteoritic sources we see today. The amount of water in the Moon is likely limited to the few hundreds of ppm (0.05–0.06 wt%) that would be soluble in a hot lunar disk at low pressures. Perhaps it is no surprise then that small amounts of water have been measured in materials from the Moon (e.g., ref. 33) indicating that the Moon-forming impactor may also have contained some water.

1. Humayun M, Clayton RN (1995) Potassium isotope cosmochemistry: Genetic implications of volatile element depletion. *Geochim Cosmochim Ac* 59:2131–2148.
2. Kleine T, et al. (2009) Hf–W chronology of the accretion and early evolution of asteroids and terrestrial planets. *Geochim Cosmochim Ac* 73:5150–5188.
3. Nyquist LE, Kleine T, Shih C-Y, Reese YD (2009) The distribution of short-lived radioisotopes in the early solar system and the chronology of asteroid accretion, differentiation, and secondary mineralization. *Geochim Cosmochim Ac* 73:5115–5136.
4. Krot AN, et al. (2009) Origin and chronology of chondritic components: a review. *Geochim Cosmochim Ac* 73:4963–4997.
5. Amelin Y (2008) The U Pb systematics of angrite Sahara 99555. *Geochim Cosmochim Ac* 72:4874–4885.
6. Touboul M, et al. (2007) Late formation and prolonged differentiation of the Moon inferred from W isotopes in lunar metals. *Nature* 450:1206–1209.
7. Weidenschilling SJ, et al. (1997) Accretional evolution of a planetesimal swarm. *Icarus* 128:429–455.
8. Ciesla FJ (2007) Dust coagulation and settling in layered protoplanetary disks. *Astrophys J* 654:L159–L162.
9. Goldreich P, Ward WR (1973) The formation of planetesimals. *Astrophys J* 183:1051–1062.
10. Weidenschilling SJ (1980) Dust to planetesimals–settling and coagulation in the solar nebula. *Icarus* 44:172–189.
11. Wetherill GW (1994) Provenance of the terrestrial planets. *Geochim Cosmochim Ac* 58:4513–4520.
12. Agnor CB, Canup RM, Levison HF (1999) On the character and consequences of large impacts in the late stage of terrestrial planet formation. *Icarus* 142:219–237.
13. Chambers JE, Wetherill GW (1998) Making the terrestrial planets: N-body integrations of planetary embryos in three dimensions. *Icarus* 136:304–327.
14. Chambers JE (1999). A hybrid symplectic integrator that permits close encounters between massive bodies. *Mon Not R Aston Soc* 304:793–799.
15. Duncan MJ, Levison HF, Lee MH (1998). A multiple time step symplectic algorithm for integrating close encounters. *AJ* 116:2067–2077.
16. O'Brien DP, Morbidelli A, Levison HF (2006) Terrestrial planet formation with strong dynamical friction. *Icarus* 184:39–58.
17. Raymond SN, Quinn T, Lunine JI (2007) High-resolution simulations of the final assembly of earth-like planets. 2. water delivery and planetary habitability. *Astrobiology* 7:66–84.
18. Raymond SN, Quinn,T, Lunine JI (2008) High-resolution simulations of the final assembly of Earth-like planets I. Terrestrial accretion and dynamics. *Icarus* 183:265–282.
19. Bromley BC, Kenyon SJ (2006) A hybrid N-body-coagulation code for planet formation. *Astron J* 131:2737–2748.
20. Righter K, Drake MJ (1997) A magma ocean on Vesta: core formation and petrogenesis of eucrites and diogenites. *Meteorit Planet Sci* 32:929–944.
21. Lodders J, Fegley B, Jr. (1997) An oxygen isotope model for the composition of Mars. *Icarus* 126:373–394.
22. Debaille V, Brandon AD, Yin QZ, Jacobsen B (2008) Martian mantle mineralogy investigated by the ^{176}Lu-^{176}Hf and ^{147}Sm-^{143}Nd systematics of shergottites. *Earth Planet Sci Lett* 269:186–199.
23. Righter K, Chabot NL (2010) Moderately and slightly siderophile element constraints on the depth and extent of melting in early Mars. *Met Planet Sc* 46:157–176.
24. Righter K (2011) Prediction of metal-silicate partition coefficients for siderophile elements: an update and assessment of PT conditions for metal-silicate equilibrium during accretion of the Earth. *Earth Planet Sci Lett* 304:158–167.
25. Halliday AN (2008) A young Moon-forming giant impact at 70–110 million years accompanied by late-stage mixing, core formation and degassing of the Earth. *Phil Trans Roy Soc London A* 366:4163–4181.
26. Wood BJ, Wade J, Kilburn MR (2008) Core formation and the oxidation state of the Earth: additional constraints from Nb, V and Cr partitioning. *Geochim Cosmochim Acta* 72:1416–1426.
27. Abe Y, et al. (2000) *Water in the early Earth. Origin of the Earth and Moon*, eds Canup RM, Righter K, (Tucson, AZ, University of Arizona Press), 413–433.
28. Morbidelli A, et al. (2000) Source regions and time scales for the delivery of water to Earth. *Meteoritics & Planetary Science* 35:1309–1320.
29. Williams Q, Hemley RJ (2001) Hydrogen in the deep Earth. *Annu Rev Earth Pl Sc* 29:365–418.
30. McCanta MC, et al. (2008) The LaPaz Icefield 04840 meteorite: mineralogy, metamorphism, and origin of an amphibole- and biotite-bearing R chondrite. *Geochim Cosmochim Ac* 72:5757–5780.
31. O'Brien DP, Morbidelli A, Levison HF (2006) Terrestrial planet formation with strong dynamical friction. *Icarus* 184:39–58.
32. Raymond SN, Quinn T, Lunine JI (2007) High-resolution simulations of the final assembly of earth-like planets. 2. water delivery and planetary habitability. *Astrobiology* 7:66–84.
33. McCubbin FM, et al. (2010) Nominally hydrous magmatism on the Moon. *Proc Nat'l Acad Sci USA* 107:11223–11228.

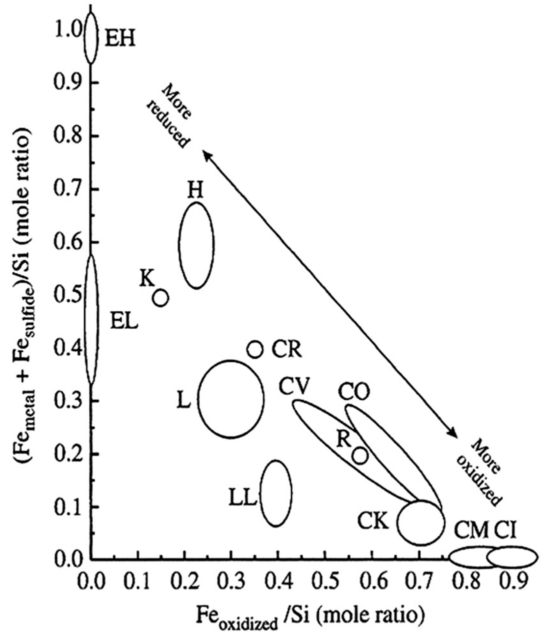

Fig. S1. The proportion of oxidized vs. reduced Fe in chondritic meteorites (from ref. 1). Abbreviations are as follows: EL and EH = enstatite chondrite groups; H, L, and LL = ordinary chondrite groups; R = R chondrites; CI, CV, CR, CM, CO, and CK are carbonaceous chondrite groups. Reprinted from Treatise on Geochemistry, Volume 1: Meteorites, Comets and Planets, A.N. Krot, K. Keil, E.R.D. Scott, C.A. Goodrich, M.K.Weisberg, 83-128, Copyright (2003) with permission from Elsevier.

1 Krot AN, Keil K, Goodrich CA, Weisberg MK, Scott ERD (2003) Classification of Meteorites.*Meteorites, Comets, and Planets*. *Treatise on Geochemistry*, ed Davis AM, (Elsevier-Pergamon, Oxford, United Kingdom), Vol. 1, 83–128. http://www.elsevier.com.

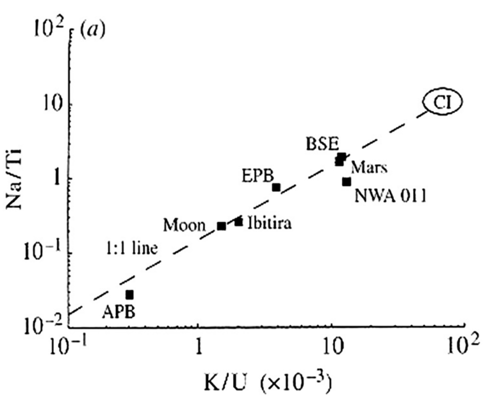

Fig. S2. Volatile element variation in planetary materials as illustrated by the Na/Ti and K/U ratios in differentiated bodies and CI chondrites (1). Reprinted from Treatise on Geochemistry, Volume 1: Meteorites, Comets and Planets, A.N. Krot, K. Keil, E.R.D. Scott, C.A. Goodrich, M.K.Weisberg, 83-128, Copyright (2003) with permission from Elsevier.

1 Krot AN, Keil K, Goodrich CA, Weisberg MK, Scott ERD (2003) Classification of Meteorites.*Meteorites, Comets, and Planets*. *Treatise on Geochemistry*, ed Davis AM, (Elsevier-Pergamon, Oxford, United Kingdom), Vol. 1, 83–128. http://www.elsevier.com.

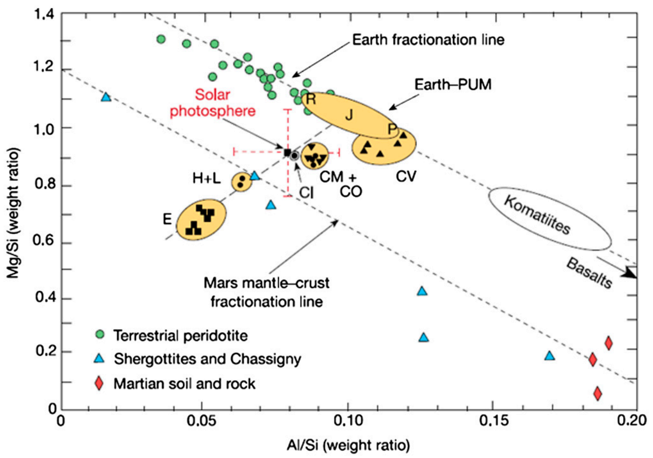

Fig. S3. The major-element composition of primitive material in the inner Solar System is not of uniform composition, but defines an unexplained trend. Mg/Si vs. Al/Si ratios in chondritic, terrestrial, and martian materials. Abbreviations are as follows: enstatite (E), ordinary (H, L), and carbonaceous (CI, CM, CO, and CV) chondrites. Dots are terrestrial peridotites, komatiites, and basalts that fall off the diagram to the right. The letters R, J, and P refer to estimates of the bulk silicate Earth composition. The martian fractionation line is defined by Chassigny, shergottites, and martian soils and rocks from the Viking and Pathinder mission. PUM, primitive upper mantle of the Earth. Figure from (1). Reproduced with permission from ref. 1 (*below*). (Copyright 2002, Nature Publishing Group).

1 Drake MJ, Righter K (2002) Determining the composition of the Earth. *Nature* 416:39–44.

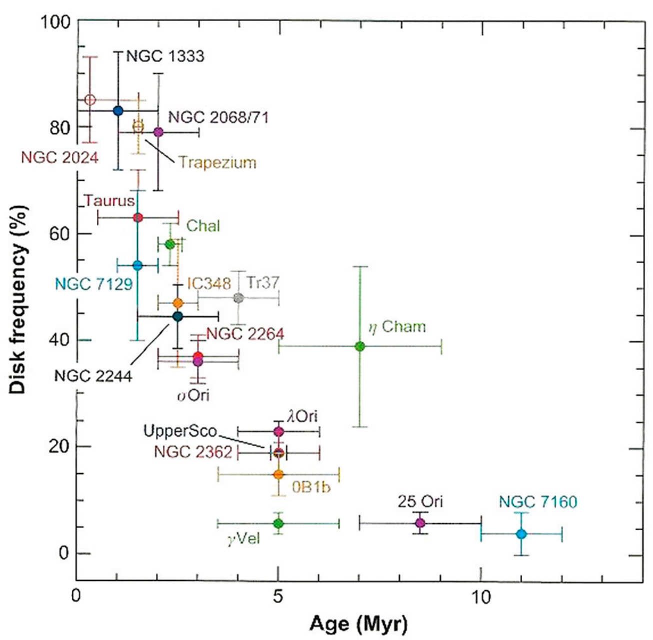

Fig. S4. Evolution of protoplanetary disks—fraction of sun-like stars with detectable near-IR excess as a function of time. Protoplanetary disks have a range of lifetimes, and most sun-like stars have lost their disks by 6 Ma after T_0 (from 1). Reproduced with permission of Annual Reviews, Inc., from Annual Review of Astronomy and Astrophysics, Wyatt, M.C., 46, 2008; permission conveyed through Copyright Clearance Center, Inc.

1 Wyatt MC (2008) Evolution of debris disks. *Annual Review of Astronomy & Astrophysics* 46:339–383.

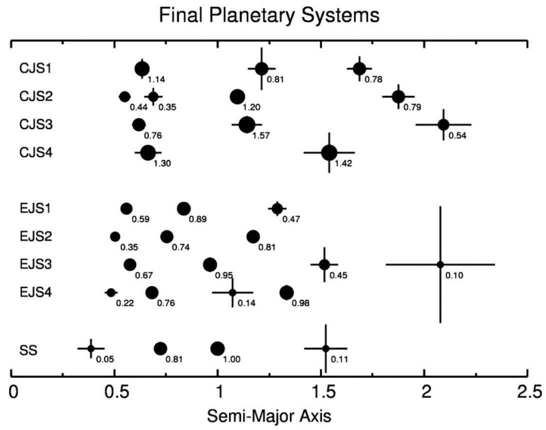

Fig. S5. Orbital configurations of the final terrestrial planets in simulations from ref. 1, where the CJS simulations were run with Jupiter and Saturn on nearly circular, low-inclination orbits and the EJS simulations were run with Jupiter and Saturn on their current, eccentric and inclined orbits. Numbers are the planet masses in Earth masses, and the lines give the range of peri/aphelion due to orbital eccentricity and the vertical range above and below the midplane due to inclination. The Solar System is shown for comparison.

1 O'Brien DP, Morbidelli A, Levison HF (2006) Terrestrial planet formation with strong dynamical friction. *Icarus* 184:39–58.

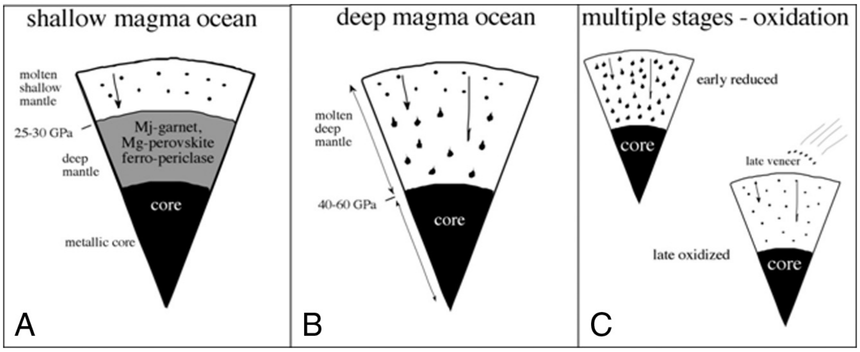

Fig. S6. Cartoon illustrating the three general types of models that have been considered in the last decade for early Earth differentiation. *A*) is an intermediate depth magma ocean, *B*) deep magma ocean, and *C*) early reduced and later oxidized magma oceans, or multistage models.

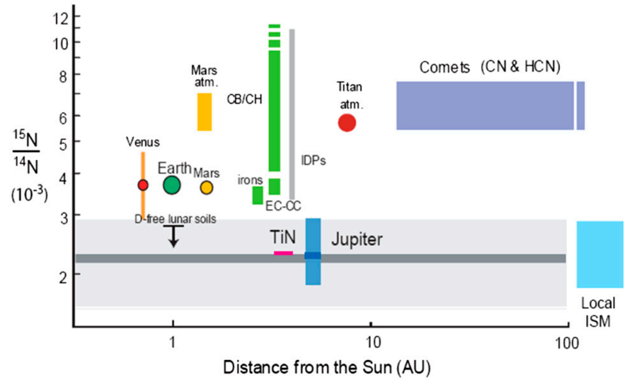

Fig. S7. Fig. 5: *N* isotopes for a large number of solar system materials showing a large variation in isotopic ratio of *N* 15/14 (from ref. 1). Reprinted from Geochimica et Cosmochimica Acta, 74, Marty, B. et al., Nitrogen isotopes in the recent solar wind from the analysis of Genesis targets: Evidence for large scale isotope heterogeneity in the early Solar system, 83-128, Copyright (2010) with permission from Elsevier.

1 Marty B, et al. (2010) Nitrogen isotopes in the recent solar wind from the analysis of Genesis targets: evidence for large scale isotope heterogeneity in the early Solar system. *Geochim Cosmochim Ac* 74:340–355 http://www.elsevier.com/wps/find/journaldescription.cws_home/212/description#description..

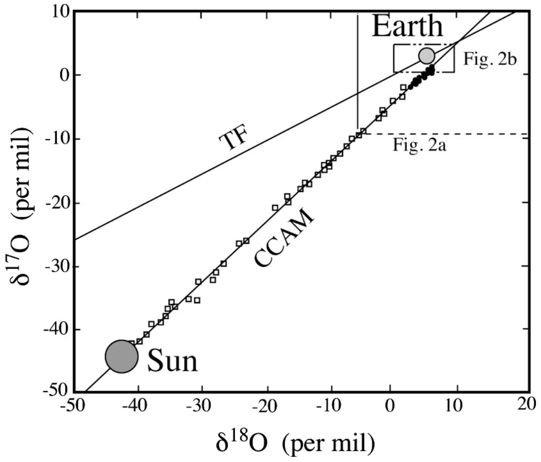

Fig. S8. Oxygen isotopic measurements of the solar wind (Sun symbol) from the Genesis mission results (from ref. 1), together with Allende matrix and dark inclusion analyses, and the location of Earth's oxygen isotopic composition which is presented in more detail in Fig. 2 *A* and *B*. CCAM is carbonaceous chondrite Allende mixing line. TF is terrestrial fractionation line.

1 McKeegan KD, et al. (2009) Oxygen isotopes in a Genesis Concentrator sample. 40th Lunar and Planetary Science Conference, Lunar and Planetary Institute, Houston, TX, abstract 2494.